Carbohydrate Polymers 245 (2020) 116566

Contents lists available at ScienceDirect

Carbohydrate Polymers

journal homepage: www.elsevier.com/locate/carbpol

Controlling the transparency and rheology of nanocellulose gels with the extent of carboxylation

David Joram Mendoza[a], Laila Hossain[a], Christine Browne[a], Vikram Singh Raghuwanshi[a], George P. Simon[b], Gil Garnier[a,*]

[a] Bioresource Processing Research Institute of Australia (BioPRIA), Department of Chemical Engineering, Monash University, Clayton, VIC 3800, Australia
[b] Department of Materials Science and Engineering, Monash University, Clayton, VIC 3800, Australia

ARTICLE INFO

Keywords:
TEMPO-periodate
Nanocellulose fibres
Nanocellulose gels
Transparency
Rheology
Superabsorbent

ABSTRACT

TEMPO and periodate are combined in a one-shot reaction to oxidise cellulose and produce nanocellulose gels with a wide range of degree of substitution (DS). Highly-oxidised cellulose nanofibres with a high charge of −80 mV were produced. The strong electrical repulsion between TEMPO-periodate oxidised nanofibres (TPOF) results in the formation of well-separated nanofibres with a diameter of 2 − 4 nm, albeit depolymerised due to high oxidation. TPOF produces highly-transparent gels due to smaller aspect ratio and high surface charge. These properties induce a reduced viscosity and moduli of the gels by decreasing fibre entanglement. TPOF gels are more stable at basic pH and high ionic strength than TEMPO-oxidised gels due to their higher surface charge. Freeze-dried TPOF gels also exhibit remarkable water holding capacity due to enhanced immobilisation of water molecules. The excellent optical properties of the highly transparent gel for red blood cells analysis open new possibilities in diagnostics application.

1. Introduction

Nanocellulose (cellulose nanocrystals, cellulose nanofibres, bacterial nanocellulose) is a biodegradable and renewable material with excellent mechanical properties, unique optical properties and tunable surface chemistry (Curvello et al., 2019; Dufresne, 2013; Habibi, 2014; Klemm et al., 2009; Nascimento et al., 2018). In particular, cellulose nanofibres (CNFs) are widely used for their inherent flexible elongated structure and their ability to form physically entangled networks at extremely low solids concentration (< 0.3 wt.%). CNFs are commonly prepared by mechanical treatments such as microfluidisation (Hietala, Ämmälä, Silvennoinen, & Liimatainen, 2016; Zimmermann, Pohler, & Geiger, 2004), ultrasound (Chen et al., 2011), high-speed blending (Uetani & Yano, 2011), twin-screw extrusion (Ho, Abe, Zimmermann, & Yano, 2015), and high-pressure homogenisation (Ämmälä, Liimatainen, Burmeister, & Niinimäki, 2013; Mendoza, Batchelor, Tabor, & Garnier, 2018). The major disadvantage of these mechanical treatments is high energy consumption. To address this issue, chemical (Isogai, Saito, & Fukuzumi, 2011; Jiang et al., 2017; Okita, Saito, & Isogai, 2010) and enzymatic (Hu, Tian, Renneckar, & Saddler, 2018; Tarres, Boufi, Mutje, & Delgado-Aguilar, 2017) pre-treatments have been explored to reduce energy consumption and minimise fibre damage.

Carboxylation or oxidation is the most common chemical pre-treatment to prepare CNFs. The introduction of negatively-charged carboxylate groups on the surface of cellulose aids in the mechanical delamination of the fibres into CNFs. Consequently, most oxidised CNFs are used as highly viscous aqueous suspensions which can form hydrogels. Indeed, carboxylated nanocellulose gels have been engineered for biomedical applications (Cheng, Park, & Hyun, 2014; Curvello et al., 2019; Curvello, Raghuwanshi, & Garnier, 2019; Zander, Dong, Steele, & Grant, 2014), drug delivery (Curvello et al., 2019; Fiorati et al., 2020), and superabsorbents (Isobe et al., 2013; Mendoza, Browne, Raghuwanshi, Simon, & Garnier, 2019).

2,2,6,6-Tetramethylpiperidine-1-oxyl (TEMPO)-mediated oxidation, coupled with mechanical fibrillation, remains as the most common method to prepare carboxylated nanocellulose gels. TEMPO is a water-soluble radical catalyst which selectively oxidises alcohol groups to aldehydes and carboxyl groups (Adam, Saha-Moller, & Ganeshpure, 2001; deNooy, Besemer, & vanBekkum, 1996). Isogai et al. have extensively studied and characterised this oxidation protocol for cellulose to prepare carboxylated nanocellulose (Isogai et al., 2011; Okita et al., 2010; Ruizhi et al., 2017; Saito & Isogai, 2004; Shinoda, Saito, Okita, & Isogai, 2012). The properties of TEMPO-oxidised nanocellulose fibres are now very well described in the literature (Isogai et al., 2011;

* Corresponding author.
E-mail address: Gil.Garnier@monash.edu (G. Garnier).

https://doi.org/10.1016/j.carbpol.2020.116566
Received 8 May 2020; Received in revised form 2 June 2020; Accepted 2 June 2020
Available online 10 June 2020

Fig. 1. One-shot TEMPO-periodate oxidation of cellulose; the priary and secondary alcohols are oxidised to carboxylate groups.

Mendoza, Batchelor et al., 2018; Mendoza, Gunawardhana, Batchelor, & Gamier, 2018). However, there is a limited range of degree of substitutions (DS) achievable with TEMPO oxidation, as only the C6 hydroxyl groups can be oxidised.

Previously, we reported a one-shot TEMPO-periodate oxidation protocol to produce carboxylated cellulose with a wide range of degree of substitution (DS) (Mendoza, Browne et al., 2019). By combining periodate with classical TEMPO-mediated oxidation, we showed that cellulose molecules with carboxylate groups in the C6, C2 and C3 positions can be prepared (Fig. 1). In this work, we hypothesise that nanocellulose gels of tunable carboxylate content and thus properties can be produced via TEMPO-periodate oxidation.

A few studies have reported changing the properties of TEMPO-oxidised fibres by manipulating the NaClO concentration (Saito, Kimura, Nishiyama, & Isogai, 2007) or the oxidation time (Benhamou, Dufresne, Magnin, Mortha, & Kaddami, 2014). However, these studies have been limited to aqueous suspensions of nanofibres, often prepared by mild disintegration such as prolonged magnetic stirring. In this study, carboxylated nanocellulose gels are prepared by high-pressure homogenisation of TEMPO-periodate oxidised cellulose fibres. We investigate how TEMPO-periodate oxidation modulates the properties of carboxylated nanocellulose gels over a wide range of carboxylate content measured as COO^-DS. It is our objective to engineer the optical, viscoelastic properties and water-absorbing capacity of nanocellulose gels by controlling the level of carboxylation. We correlate these properties with the structure of the nanocellulose fibres with varying DS. We also highlight how the surface charge affects the stability of these gels at varying pH and ionic strength. Last, the potential of TEMPO-periodate oxidised gels as matrix for red blood cell analysis and diagnostics is demonstrated. We show that TEMPO-periodate oxidation provides high transparency of the gels enabling improved imaging of red blood cells. The excellent transparency of the nanocellulose gel opens new possibilities in gel card-based blood diagnostics. This study aims to engineer nanocellulose gel properties by controlling the level of carboxylation using a combination of TEMPO and periodate oxidation.

2. Materials and methods

2.1. Materials

Never-dried Bleached Eucalyptus Kraft (BEK) pulp of approximately 10 wt.% solids content, was supplied by Australian Paper, Maryvale, Australia. Sodium periodate ($NaIO_4$), 2,2,6,6-tetramethylpiperidine-1-oxyl (TEMPO), and sodium bromide (NaBr) were purchased from Sigma-Aldrich (NSW, Australia). 12 w/v% sodium hypochlorite (NaClO) was purchased from Thermo Fisher Scientific. All chemicals are analytical grade and used without further purification. All materials expressed in mmol/g refer to the dry mass of cellulose.

2.2. Synthesis of carboxylated nanocellulose gels

TEMPO-periodate oxidation of cellulose was based on studies reported previously (Baron et al., 2019; Coseri et al., 2015; Mendoza, Hossain et al., 2019). Approximately 10 g (dry mass basis) of disintegrated BEK pulp was suspended in 1200 mL distilled water containing TEMPO (0.5 mmol/g), NaBr (8.0 mmol/g), and $NaIO_4$(0.1–5 mmol/g). The reaction vessel was covered with aluminium foil to prevent any photoinduced decomposition of periodate. NaClO (12% v/v, pH 10.5, 8 mmol/g) was then added dropwise and the pH was maintained at 10.5 using 0.5 M NaOH. After 4 h, the oxidation reaction was stopped by quenching with 10 mL ethanol. The oxidised fibres were vacuum filtered and washed several times with distilled water until neutral pH was achieved, with the fibres then freeze-dried for 48 h. For comparison, cellulose oxidised with TEMPO/NaBr/NaClO (0 mmol/g $NaIO_4$) was also prepared.

Different solid concentrations of the oxidised fibres (0.1 wt.% to 1.0 wt.%) were prepared by suspending known amounts of the oxidised fibres in water. The suspensions were passed through a high-pressure homogeniser (GEA Niro Soavi Homogeniser Panda) at 1000 bar to produce TEMPO-periodate oxidised (TPOF) and TEMPO oxidised (TOF) nanocellulose gels. Suspensions with less than 1 wt.% were homogenised by two passes, while samples with concentrations greater than 1 wt.% were homogenised using one pass only.

2.3. Characterisation of carboxylated nanocellulose gels

2.3.1. Fourier-transform infrared (FTIR) spectroscopy

Freeze-dried nanofibres were analysed with a Fourier Transform Infrared (FTIR) spectrometer (Agilent Technologies Cary 630 FTIR) equipped with a diamond attenuated total reflectance (ATR) accessory. Eight scans at 4 cm^{-1} resolution were recorded in the range of $4000-500\ cm^{-1}$.

2.3.2. Carboxylate content and degree of substitution (DS)

The carboxylate content and degree of substitution were quantified by conductimetric titration as reported previously (Curvello et al., 2019; Mendoza, Batchelor et al., 2018; Perez, Montanari, & Vignon, 2003). Freeze-dried oxidised nanofibres (ca. 0.1 g) were dispersed in 40 mLl of Milli-Q water. 200 μL of 0.1% NaCl was then added and the pH was adjusted to 2.5 using 0.5 M HCl. Conductimetric titration was performed using a 0.1 N NaOH as titrant operating at a rate of 0.1 mL/min (Mettler Toledo T5 titrator). The carboxylate content (mmol COO^-/g fibre) was calculated by Eq. 1:

$$Carboxylate\ content\left(mmol\ COO^{-}/g\right) = \frac{C\,(V_2 - V_1)}{w} \times 1000 \quad (1)$$

where V_2 and V_1 are the volume of titrant required to neutralise the carboxylic groups, C is the NaOH concentration (M), and w is the dry sample weight.

DS is expressed as the ratio of the amount of the sodium carboxylate groups and the total hydroxyl groups in the anhydroglucose unit (AGU). The degree of substitution was calculated by the following equation:

$$Degree\ of\ Substitution = \frac{162 \times C \times (V_2 - V_1)}{w - 111 \times C \times (V_2 - V_1)} \times 100 \quad (2)$$

where V_2 and V_1 are the volume of titrant required to neutralise the carboxylic groups, C is the NaOH concentration (M), w is the dry sample weight and 111 is the molar mass difference of 2,3,6-tricarboxycellulose and AGU.

2.3.3. Degree of polymerisation

The average viscometric degree of polymerisation(DP_v) of the cellulose nanofibres was quantified, as previously reported (Haun, Yoon, Lee, & Weissleder, 2010; Shinoda et al., 2012). About 0.25 g of the oxidised nanofibres were dissolved in 50 mL of 0.5 M copper ethylenediamine for 30 min. The intrinsic viscosities were then measured using a Cannon − Fenske capillary viscometer. These values were converted to DP_v with the Mark − Houwink − Sakurada equation (Saito

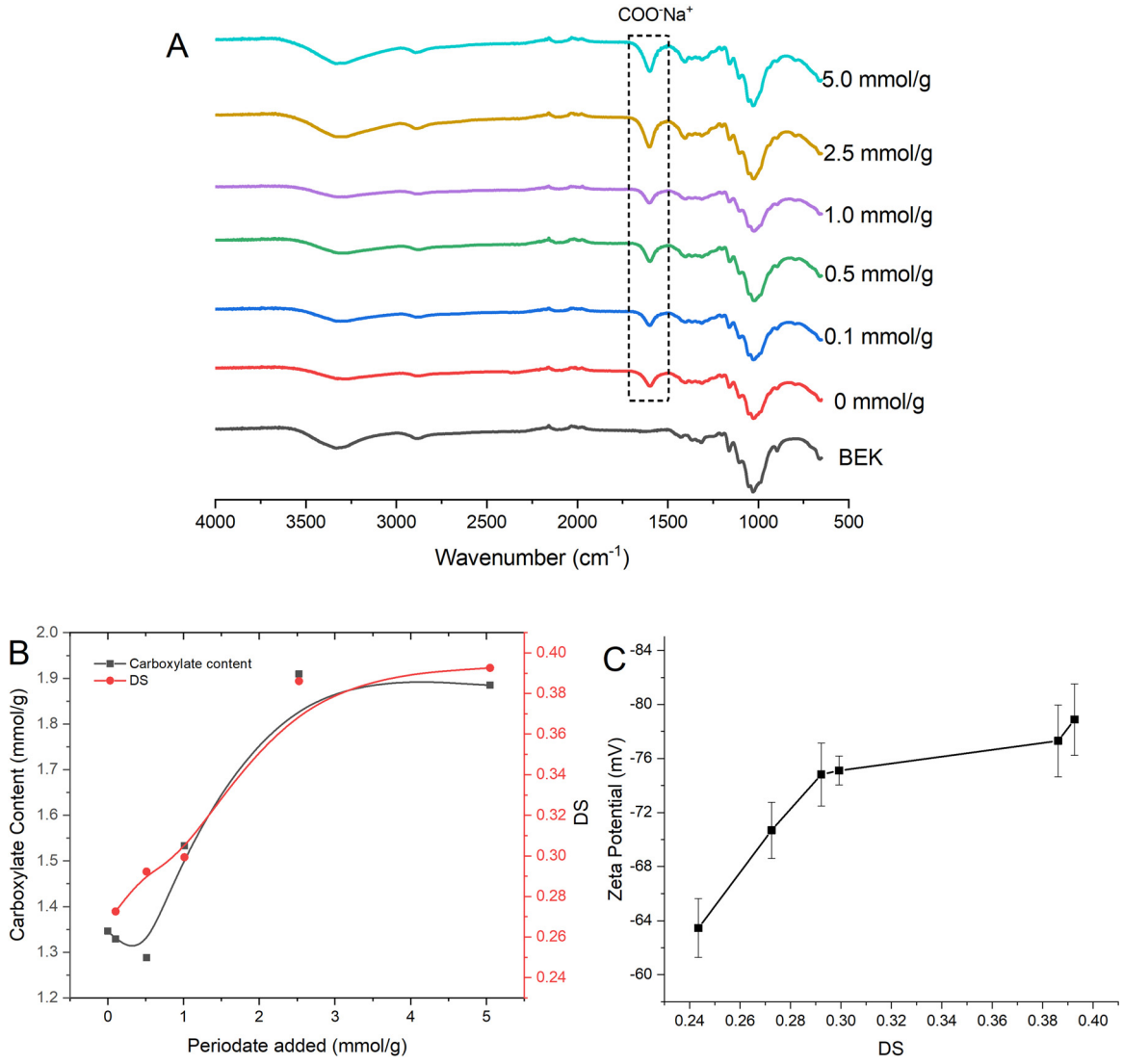

Fig. 2. (a) FTIR spectra of BEK and TEMPO-periodate oxidised nanocellulose at varying periodate concentrations. **(b)** Effect of periodate concentration on the carboxylate content and DS of oxidised nanocellulose gels. **(c)** Effect of DS on the zeta potential of nanocellulose fibres.

et al., 2009), where [ŋ] is the average intrinsic viscosity measured from three replicates:

$$[\eta] = 0.57 \times DP_v \quad (3)$$

2.3.4. Zeta potential

The zeta potential of nanocellulose fibres was measured as previously reported (Okita et al., 2010). Dilute suspensions of the gels (~0.01%) were sonicated for 2 min using an ultrasonic homogeniser at 19.5 kHz and 70% amplitude (ON/OFF, 5 s). Larger fibres were then separated by centrifugation at 12,000 *g* for 5 min. The zeta potential of the supernatants was the average of five measurements using a zeta potential analyser (Brookhaven Nanobrook Omni).

2.3.5. UV–vis spectroscopy

Transmittance spectra of 1 wt.% gels were generated at 300 − 800 nm using a UV–vis spectrometer (Cary 60 UV–vis Agilent Technologies). Prior to analysis, the gels were centrifuged at 4000 rpm to remove any trapped bubbles.

2.3.6. Rheology studies

Rheological testing of the nanocellulose gels was based on methods reported previously (Mendoza, Batchelor et al., 2018; Mendoza, Batchelor et al., 2018). An Anton Paar MCR302 rheometer, equipped with a cone (0.997°) and plate (49.975 mm) geometry, was used. Viscosity measurements were performed at a shear rate ranging from 0.5–100 s^{-1}. Oscillatory strain sweep was measured from 0.01–100% at a constant frequency (1 Hz). All measurements were performed in triplicates at ambient temperature (25 °C).

2.3.7. Transmission electron microscopy (TEM)

Transmission Electron Microscopy (TEM) was performed using a FEI Tecnai F20. Dilute suspensions of the gels (~ 0.001%) were sonicated with an ultrasonic probe at 70% amplitude for 2 min and were allowed to dry on plasma-cleaned copper grids. The samples were then stained with 2% uranyl acetate, air dried, and examined at 200 kV.

2.3.8. Free swell capacity (FSC)

Freeze-dried nanocellulose gels were placed in a funnel and submerged in deionised water for reabsorption. The water absorbed was measured by weighing the gels at regular intervals up to 92 h. Prior to weighing, the gels were allowed to stand on an inclined surface for five minutes for the excess liquid to run off. The free swell capacity (FSC) is calculated using the following equation:

$$FSC = \frac{m_f - m_i}{m_i} \quad (4)$$

where m_f is the mass of the swollen gel at a particular time and m_i is the initial mass of the gel. All measurements were performed in triplicate.

2.4. Loading of red blood cells on nanocellulose gels

Glycine (300 mM) was dissolved into the gel to balance the osmolality to physiological levels. Reagent red blood cells (3%, AHG Control Cells, Immulab) were diluted in PBS, making up an 0.8% concentration. A volume of 50 μL of the gel was placed on a glass slide and 20 μL of RBCs were loaded in TPOF gels. The RBCs were imaged under an optical microscope (Nikon Eclipse Ni-E Upright Microscope) at 100X magnification.

2.5. Effect of pH and salt concentration on nanocellulose gels

The effect of pH and salt concentration on the stability of 1 wt.% TOF and TPOF gels were determined qualitatively. The pH of the gels was varied from 2–12.5 by the addition of 0.5 M NaOH or 1 M HCl. The salt content of the gels was varied from 0–68.5 mM by adding 3 M NaCl. The gels were then centrifuged at 4,000 rpm for 20 min to separate any released water. The ratio between the initial and final gel height was calculated and expressed as the fibre ratio.

3. Results

3.1. Surface charge

The concentration of carboxylate groups on nanocellulose was determined by FTIR analysis and conductimetric titration. Fig. 2a shows the FTIR spectra of native cellulose and TEMPO-periodate oxidised nanocellulose fibres at varying periodate concentrations. The typical cellulose peaks are observed in all samples: a broad O−H stretching at 3300 cm^{-1} and an sp^3-hybridized C–H stretching at 2900 cm^{-1}(Dufresne, 2012). However, the intensity of these peaks is relatively weak in all TEMPO-periodate oxidised nanocellulose. All oxidised samples show low peak intensities at 1000−1060 cm^{-1}(C−O−C-stretching vibrations), 1201 cm^{-1} (−OH in-plane bending), 1112 cm^{-1} (C−H deformation stretching vibration), and 1165 cm^{-1} (asymmetry stretch vibration), which suggests that some degradation has occurred. The formation of sodium carboxylate groups in all oxidised nanocellulose is shown by the presence of a sharp peak at 1615 cm^{-1}. In general, this sharp peak increases with increasing periodate concentration.

High levels of carboxylate groups (1.27–1.94 mmol COO^-/g fibre) were introduced on nanocellulose by oxidative reactions (Fig. 2b). The carboxylate content and degree of substitution of the nanocellulose fibres increase with periodate concentration. An abrupt increase in carboxylate content and DS is observed at 2.5 mmol/g periodate. This increase in COOH substitution, expressed as DS, increases the nanocellulose charge as measured by zeta potential (Fig. 2c). Interestingly, the TEMPO-periodate oxidised cellulose nanofibres have a significant surface charge, as high as −80 mV.

3.1.1. Optical transmittance

TEMPO and TEMPO-periodate oxidised nanocellulose gels (1 wt.%) of varying carboxylate content were produced (Fig. 3). These gels range from translucent to highly transparent. The gel optical transmittance at 715 nm increases with the level of periodate concentration in the oxidation reaction. The difference in optical transmittance between TOF gel (7%) and TPOF gel (as high as 65%) is significant. DS directly affects the optical transmittance of the gel (Fig. 3); nanocellulose gels transparency increases non-linearly with DS or the level of oxidation.

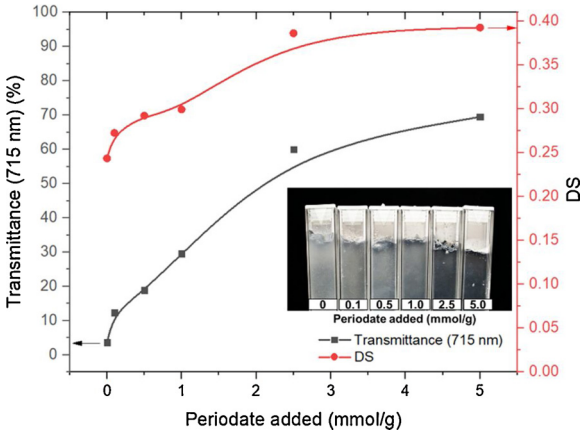

Fig. 3. Effect of periodate concentration on DS and optical transmittance of 1 wt.% nanocellulose gels at 715 nm. Inset: photographs of the oxidised nanocellulose gels.

3.1.2. Morphology and degree of polymerisation

Fig. 4 shows the transmission electron micrographs (TEM) of TEMPO-oxidised (0 mmol IO_4^-/g) and TEMPO-periodate oxidised (2.5 mmol IO_4^-/g) nanocellulose fibres. The oxidised celluloses were fully disintegrated into nanofibres with measured widths less than 4 nm, agreeing with previous reports (Shinoda et al., 2012). Interestingly, TEMPO-oxidation produced long and aggregated nanofibres (> 1 μm long, > 5 nm wide), whereas TEMPO-periodate oxidation led to shorter and better separated individualised nanofibres (< 0.5 μm long, 2−4 nm wide).

The effect of oxidation on the cellulose degree of polymerization (DP) was measured by viscosity. The nanocellulose degree of polymerisation degrades faster than linearly with DS (Fig. 5). A gradual and linear decrease in the DP_v of nanofibres is initially observed for DS ranging from 0.24 to 0.30, followed by a step decrease for DS > 0.30. These results support the TEM analysis; that is, increasing the level of oxidation increases charge density but shortens nanofibres. This corroborates a previous study where the fibril length of TEMPO-oxidised fibres decreased with increasing NaClO concentration (Shinoda et al., 2012). However, because the DS range investigated in this study is much wider than previously reported, cellulose nanofibres of lower fibril length and DP_v are achieved.

3.1.3. Viscoelastic properties

Rheology measured the effects TEMPO-periodate oxidation has on the viscoelastic properties of nanocellulose gels. The viscosity curves of TEMPO (TOF; 0 mmol IO_4^-/g) and TEMPO-periodate (TPOF; 2.5 mmol IO_4^-/g) oxidized nanocellulose gels are presented at different concentration in Fig. 6a. All gels exhibited shear-thinning behaviour: viscosity decreases with an increase in shear rate. This corroborates previous work on TEMPO-oxidised gels (Curvello et al., 2019; Mendoza, Batchelor et al., 2018; Mendoza, Batchelor et al., 2018), but innovates in increasing the carboxylate content or DS tested. TOF gels have a higher zero shear viscosity than TPOF gels at 0.5 and 1 wt.% concentration. The dynamic moduli (G' and G'') of the nanocellulose gels are quantified by oscillatory measurements (Fig. 6b). G' describes the dynamic elasticity or solid-like behaviour of the material, while G'' is the viscous modulus or the liquid-like behaviour. The strength of TOF and TPOF gels increases with increasing solids concentration. At 0.1 to 0.5 wt.%, TOF gels possess higher dynamic modulus compared to their TPOF counterparts; however, the opposite trend is observed at 1 wt.%.

To understand the opposite trend at 1 wt.%, the effect of periodate concentration and DS on the viscoelastic properties at this concentration was investigated. Fig. 7 reveals that TPOF gels (0.1–5.0 mmol/g IO_4^-) exhibit higher zero-shear viscosity (Fig. 7a) and dynamic moduli (Fig. 7b) than TOF gel (0 mmol/g IO_4^-), confirming the results of

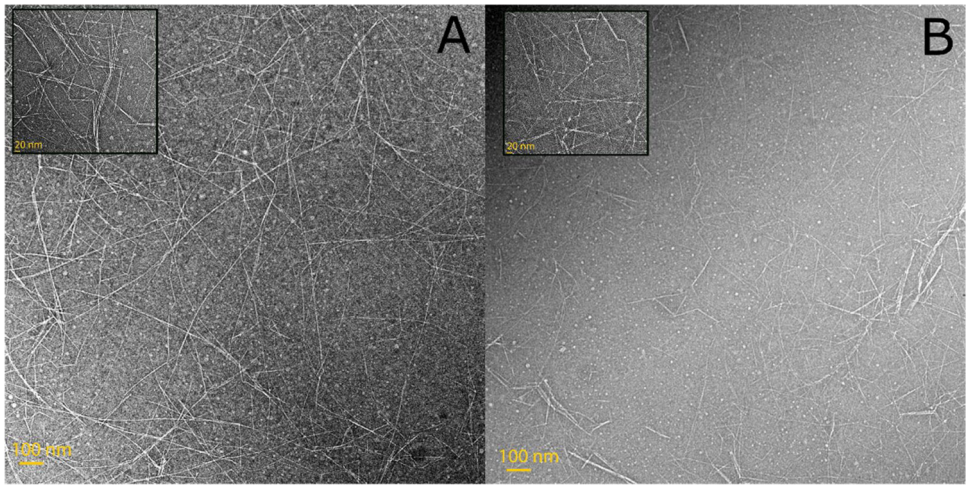

Fig. 4. TEM images of **(a)** TEMPO oxidised cellulose nanofibres (TOF) and **(b)** TEMPO-periodate oxidised nanofibres (TPOF).

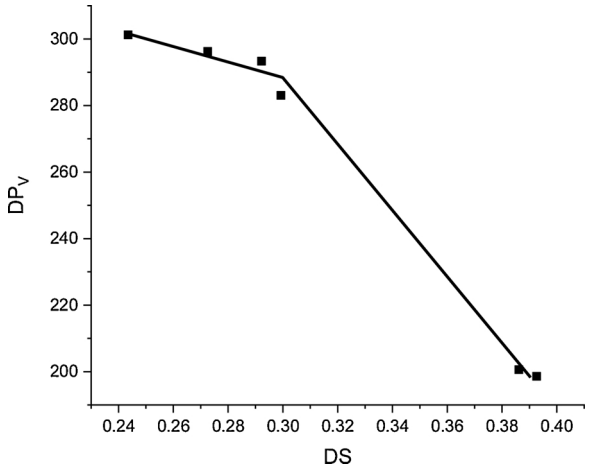

Fig. 5. Effect of the DS on the average viscometric degree of polymerisation (DP_v) of TEMPO-periodate oxidised nanocellulose fibres.

Fig. 6. However, such increases do show a maximum; the gel viscosity and strength started to marginally decrease at DS = 0.30. However, 1 wt.% TPOF gels of DS = 0.38 − 0.4 exhibit higher viscosity and dynamic moduli than 1 wt.% TOF gel (DS = 0.24). This suggests that DS does not correlate linearly with the viscoelastic properties of carboxylated nanocellulose gels; viscosity and dynamic moduli of the gels are influenced by factors such as solids concentration, aspect ratio, and DS.

3.1.4. Effect of pH and salt concentration on stability

Fig. 8 shows the effect of salt and pH on the stability of 1 wt.% TOF and TPOF gels. The gel stability was quantified with the fibre ratio defined as the gel height after over that before pH and salt treatment. Fig. 8a reveals that TPOF gels remain stable up to 40 mM NaCl, whereas TOF gels release water at only 20 mM NaCl. Both TOF and TPOF gels are unstable under acidic pH but stable over pH ranging from 7 to 11 (Fig. 8b). Interestingly, at pH = 12.5, TPOF gels remain relatively stable, whereas TOF gels released a significant amount of water (fibre ratio = 0.5).

3.1.5. Free swell capacity (FSC)

Carboxylated nanocellulose gels were freeze-dried and their water reabsorption capacity measured. The swelling profile and free swell capacity of the gels at equilibrium are shown in Fig. 9. The swelling of all freeze-dried gels is characterised by an initial abrupt absorption of water during the first 10 h, followed by sustained retention of water until equilibrium (92 h). This study supports previous results (Curvello et al., 2019), but broadens the findings over a much wider range of charge. Consistently, nanocellulose gels treated with higher periodate

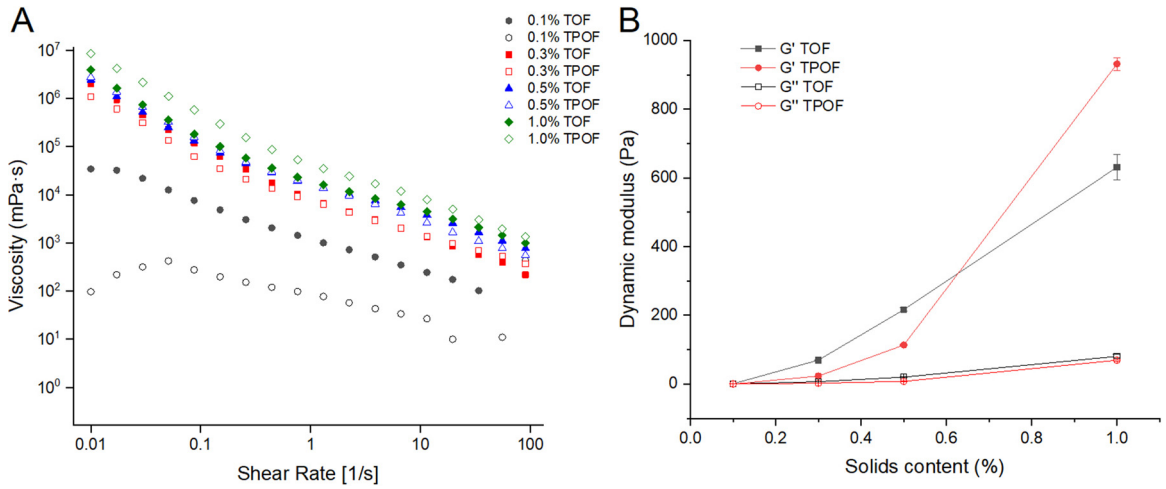

Fig. 6. (a) Viscosity curves of TOF (0 mmol IO_4^-/g) and TPOF (2.5 mmol IO_4^-/g) nanocellulose gels as a function of solids concentration (wt.%). **(b)** Dynamic moduli (Pa) of TOF (0 mmol/g IO_4^-) and TPOF (2.5 mmol/g IO_4^-) gels at different concentrations (wt. %). Measurements were performed at 25 °C and constant frequency (1 Hz). Filled and unfilled symbols represent G' and G'', respectively.

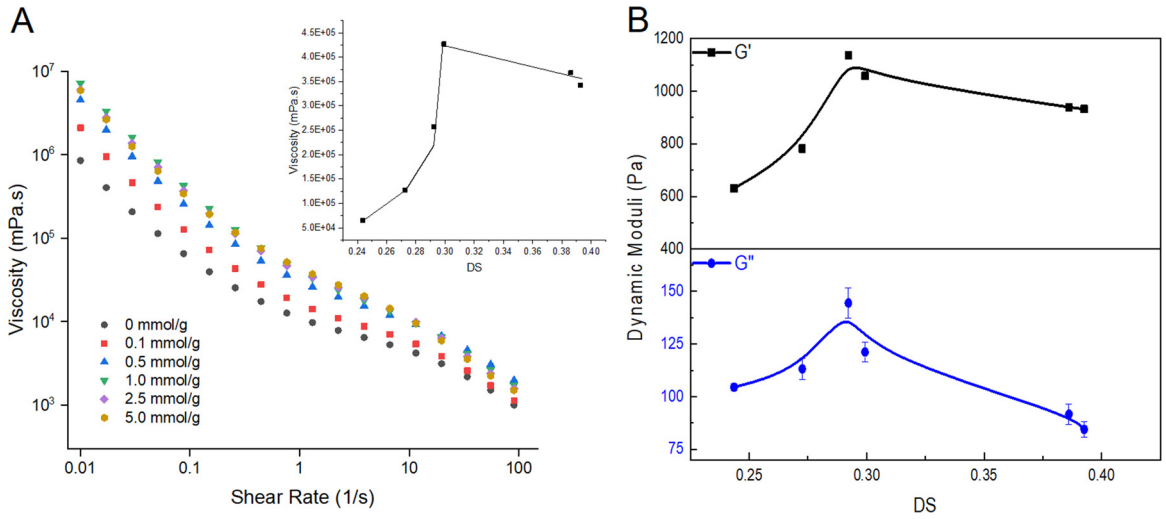

Fig. 7. (a) Viscosity curves of carboxylated nanocellulose gels as a function of periodate concentration (mmol/g). Inset shows the effect of DS on the viscosity of the gels at 0.1 s^{-1}. **(b)** Dynamic moduli (Pa) of carboxylated nanocellulose gels as a function of DS. Measurements were performed at 25 °C and constant frequency (1 Hz). Filled and unfilled symbols represent G' and G", respectively.

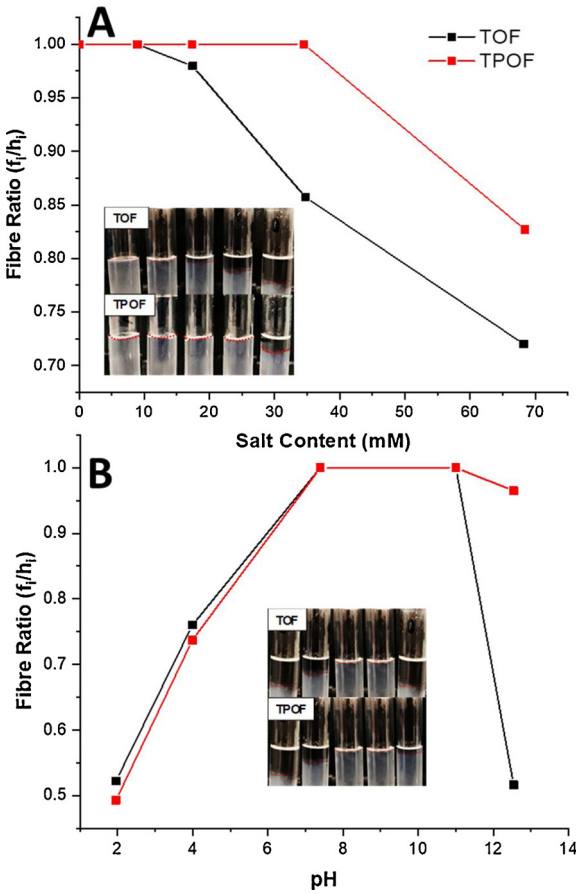

Fig. 8. The effect of **(a)** salt content (mM) and **(b)** pH on the stability of 1 wt.% TOF and TPOF gels. Insets show the release of water from the gels at pH (2-12.5) and salt levels (0-70 mM NaCl).

concentration exhibit a higher FSC. At equilibrium, nanocellulose gels free swell capacity (FSC) increases linearly with DS.

3.1.6. Red blood cells in nanocellulose gels

Reagent red blood cells were loaded in 0.3 wt.% TEMPO-periodate oxidised gels and imaged by optical microscopy. Healthy red blood cells can clearly be imaged in the transparent TPOF gel (Fig. 10). This demonstrates the potential of the gel as a biocompatible media as a matrix for cell imaging and diagnostic application. The high transparency of the gel is attributed to the high oxidation level in TEMPO-periodate oxidation which may not be achievable with TEMPO oxidation alone or mechanical and enzymatic treatments.

4. Discussion

TEMPO-mediated oxidation is the most common chemical pretreatment to carboxylate cellulose and liberate cellulose nanofibres upon homogenisation. However, the COOH substitution can exclusively occur in the C6 glycosidic position, which limits the degree of substitution achievable in carboxylated nanocellulose. In this study, TEMPO-mediated oxidation is combined with periodate in a one-shot reaction to carboxylate cellulose. FTIR and conductimetric titration analyses (Fig. 2) reveal that the addition of periodate controls the level of nanocellulose carboxylation. COOH substitution is higher in TEMPO-periodate oxidation than TEMPO oxidation as evidenced by the significant increase in surface charge (−80 mV) for TPOF nanofibres. This is the most stable and highly-charged nanocellulose fibre that we have prepared to date. This is expected in TEMPO-periodate oxidation, as the C2, C3, and C6 hydroxyl groups can be oxidised to carboxylate groups (Fig. 1). The greater surface charge in TPOF enables a significant increase in the degree of nanofibrillation, as revealed by TEM. The stronger electrical repulsion and decreased hydrogen bonding in TPOF enhanced nanofibrillation relative to TOF. However, at high DS, TPOF fibres start to degrade as indicated by the decrease in DP_v and length (Figs. 4 and 5).

The remarkable increase in surface charge and enhanced nanofibrillation enable the good dispersion of the nanofibres in water to form a gel. The characteristics of the gel are directly associated with the extent of carboxylation of the nanofibrils. Here, we correlate the properties of the nanofibres with the gel transparency, salt and pH stability, rheology, and water absorbency.

Because of the higher charge and better fibrillation in TEMPO-periodate oxidation, the resulting gels are highly transparent (Fig. 3). The strong electrical repulsion between the TPOF fibres hinder their aggregation and thus reduce the light scattering of the gels (Saito et al., 2007). The high transparency of the nanofibres is also attributed to their lower aspect ratio (Carr, Shen, & Hermans, 1977; Carr & Hermans, 1978); that is, the width of the nanofibres are smaller than the wavelength of light which causes the gels to be transparent.

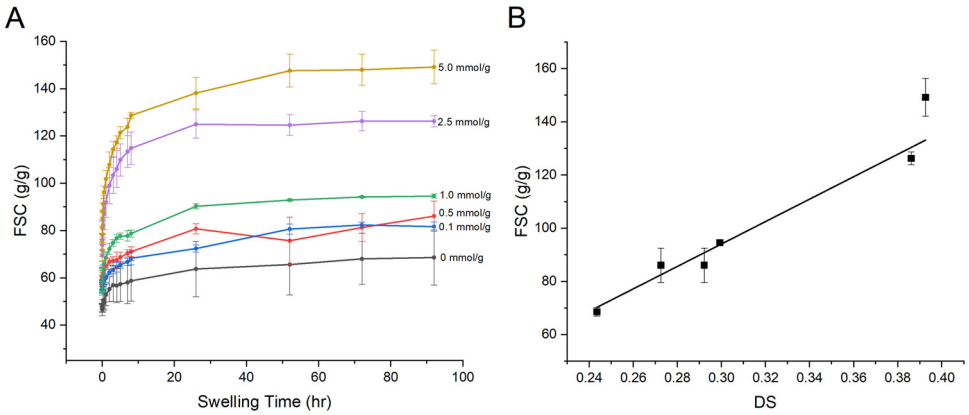

Fig. 9. (a) Swelling profile of 1 wt.% freeze-dried carboxylated nanocellulose gels at different periodate concentrations (mmol/g) in water. **(b)**Free swell capacity of freeze-dried carboxylated nanocellulose gels with different DS at equilibrium (92 h).

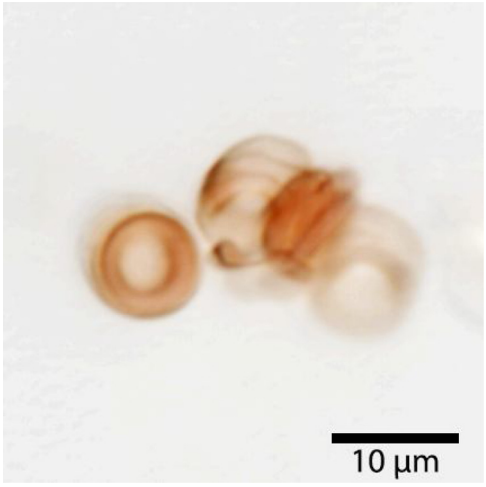

Fig. 10. Optical image of red blood cells in 0.3 wt.% TEMPO-periodate nanocellulose gels at 100x magnification.

The lower aspect ratio and higher surface charge of TPOF nanofibres also explain the reduced viscosity and moduli TPOF gels at 0.1 − 0.5 wt. % (Figs. 6 and 7). At high DS, the nanofibrils are significantly shorter and the probability of fibre entanglement in a dilute suspension is also decreased; resulting in the formation of weakly-networked gels (Benhamou et al., 2014), such as in the case of TPOF gels at 0.1 − 0.5 wt.%. We hypothesise that these fibrils behave like cellulose nanocrystals assembled as liquid crystals where fibre entanglement is limited and repulsive forces are dominant (Urena-Benavides, Ao, Davis, & Kitchens, 2011). These rigid rods tend to percolate and form a gel. Conversely, at 1 wt.%, TPOF gels become stiffer than TOF gels. This is due to the higher fibrillation level resulting from enhanced electrical repulsion leading to a stronger network. However, as seen in Fig. 7, this is only true at DS $\leq$ 0.3. The gradual decrease in moduli and viscosity with DS is attributed to the lower agglomeration ability of the nanofibres due to higher electrical repulsion (Benhamou et al., 2014; Geng et al., 2018).

The higher charge of TPOF nanofibres also explains the enhanced stability of TPOF gels relative to TOF gels at elevated pH and salt levels (Fig. 8). Increasing the ionic strength effectively screens the negatively-charged carboxylate groups which also decreases the electrical double layer in gels. This results in the destabilisation of the colloidal system and ultimately leads to the collapse of the existing fibre network (Mendoza, Batchelor et al., 2018). TPOF gels, having a higher surface charge than TOF gels, require a greater concentration of salt ions to screen the nanocellulose surface charges. On the other hand, pH severely affects the stability of carboxylated nanocellulose gels. At low pH, the carboxylate groups are protonated resulting in decreased surface potential and electrical repulsion, leading to fibre agglomeration and gel destabilisation (Mendoza, Batchelor et al., 2018). Both TOF and TPOF gels exhibit the same behaviour at acidic and slightly basic conditions. Carboxylated gels are relatively stable at basic pH; however, the effect of ionic strength also needs to be considered. Only the TPOF gel remains stable at pH = 12.5. This is because the ionic strength at pH 12.5 is sufficient to cause TOF gel to collapse.

Increasing the DS of the gels also improves their water holding capacity (Fig. 9). Gels bearing a higher DS or more carboxylate groups can immobilise more water molecules by hydrogen bonding (Hossain et al., 2020; Mendoza, Browne et al., 2019). At 5 mmol IO_4^-/g, the FSC of 1 wt.% TPOF gel is reported to be as much as 150 g/g, which is comparable with commercial superabsorbent polymers such as potassium polyacrylate (Zhang, Feng, & Jin, 2020). TPOF foams can be developed as a green alternative to the current petrochemical-based, irritant and even toxic superabsorbent.

In summary, combining periodate with TEMPO oxidation enables the control of the degree of substitution and surface charge of nanocellulose fibres. Increasing the level of oxidation increases the surface charge and degree of nanofibrillation. However, the nanofibres depolymerise as a consequence of high degree of oxidation (Isogai et al., 2011; Shinoda et al., 2012). The enhanced nanofibrillation, in addition to higher charge, results in very stable and homogeneous nanofibrils forming the gel. These gels are more transparent and exhibit better water-holding capacity and pH and salt stability. High degree of oxidation also induces reduced viscosity and dynamic moduli. The rheology of these gels resembles that of cellulose nanocrystals exhibiting liquid crystal behaviour where electrical repulsion is dominant and fibre entanglement is limited. By controlling the extent of carboxylation of cellulose, we can manipulate the properties of carboxylated nanocellulose gels.

To demonstrate the potential application of the highly transparent gel, we loaded reagent red blood cells and use it as a matrix for storage and analysis. Fig. 10 reveals that red blood cells remain healthy and can be directly imaged whilst loaded inside the gel. The high transparency of the gel allowed clear imaging of the red blood cells. The transparency or cloudiness of the gel is particularly important for imaging and ophthalmic applications (Wang & Han, 2017). The excellent transparency of the nanocellulose gel open new possibilities in diagnostics application.

5. Conclusion

2,2,6,6-Tetramethylpiperidine-1-oxyl (TEMPO)-mediated oxidation coupled with mechanical fibrillation remains as the most common

method to prepare carboxylated cellulose nanofibres. However, the degree of substitution (DS) achievable is limited as only the C6 hydroxyl groups can be oxidised. In this work, TEMPO and periodate are combined in a one-shot reaction to oxidise the C2, C3, and C6 OH groups and produce nanocellulose gels over a wide range of DS. TEMPO-periodate oxidation yields highly-carboxylated cellulose nanofibres (DS = 0.4) with a very high charge of −80 mV. The strong electrical repulsion between the fibres results in the formation of well-separated nanofibres with a diameter of 2−4 nm, although depolymerisation is observed as a consequence of the high oxidation level.

The properties of the gels can be engineered through TEMPO-periodate oxidation/fibrillation. TEMPO-periodate oxidised fibres (TPOF) results in a highly-transparent gel. Their smaller aspect ratio and very high surface charge prevents aggregation and reduces the light scattering of the gels. TEMPO-periodate oxidation also results in gels of reduced viscosity and dynamic moduli. Gel rheology is dependent on the DS and nanofibre concentration. In a dilute regime (0.1−0.5 wt.%), TPOF nanofibres have a low tendency to entangle to form a strong network due to strong electrical repulsion and reduced length. At 1 wt. %, these fibres form a stronger network thanks to an enhanced degree of fibrillation. The TPOF gels have a superior stability at basic pH and high ionic strength due to their high surface charge. Freeze-dried nanocellulose foams prepared from TPOF gels also exhibit remarkable water holding capacity and can immobilise more water molecules by hydrogen bonding. The potential of the highly transparent gel for red blood cells analysis and diagnostic applications is also demonstrated.

CRediT authorship contribution statement

David Joram Mendoza: Conceptualization, Validation, Methodology, Investigation, Software, Writing - original draft. **Laila Hossain:** Methodology, Investigation, Writing - original draft. **Christine Browne:** Validation, Writing - review & editing. **Vikram Singh Raghuwanshi:** Validation, Writing - review & editing. **George P. Simon:** Supervision, Writing - review & editing. **Gil Garnier:** Visualization, Supervision, Writing - review & editing.

Acknowledgements

Funding from the Australian Research Council-Industry Transformation Research Hub; Processing Advanced Lignocellulosics (PALS) [grant number IH170100020] is gratefully acknowledged. Many thanks to Dr. T. Williams, Monash Centre for Electron Microscopy (MCEM), for assistance in TEM analysis and Mr. R Curvello and Ms. D. Alves for help with red blood cells experiment.

References

Adam, W., Saha-Moller, C. R., & Ganeshpure, P. A. (2001). Synthetic applications of nonmetal catalysts for homogeneous oxidations. *Chemical Reviews, 101*(11), 3499–3548.

Ämmälä, A., Liimatainen, H., Burmeister, C., & Niinimäki, J. (2013). Effect of tempo and periodate-chlorite oxidized nanofibrils on ground calcium carbonate flocculation and retention in sheet forming and on the physical properties of sheets. *Cellulose, 20*(5), 2451–2460.

Baron, R. I., Bercea, M., Avadanei, M., Lisa, G., Biliuta, G., & Coseri, S. (2019). Green route for the fabrication of self-healable hydrogels based on tricarboxy cellulose and poly(vinyl alcohol). *International Journal of Biological Macromolecules, 123*, 744–751.

Benhamou, K., Dufresne, A., Magnin, A., Mortha, G., & Kaddami, H. (2014). Control of size and viscoelastic properties of nanofibrillated cellulose from palm tree by varying the TEMPO-mediated oxidation time. *Carbohydrate Polymers, 99*, 74–83.

Carr, M. E., & Hermans, J. (1978). Size and density of fibrin fibers from turbidity. *Macromolecules, 11*(1), 46–50.

Carr, M. E., Jr, Shen, L. L., & Hermans, J. (1977). Mass–length ratio of fibrin fibers from gel permeation and light scattering. *Biopolymers, 16*(1), 1–15.

Chen, W. S., Yu, H. P., Liu, Y. X., Chen, P., Zhang, M. X., & Hai, Y. F. (2011). Individualization of cellulose nanofibers from wood using high-intensity ultrasonication combined with chemical pretreatments. *Carbohydrate Polymers, 83*(4), 1804–1811.

Cheng, J., Park, M., & Hyun, J. (2014). Thermoresponsive hybrid hydrogel of oxidized nanocellulose using a polypeptide crosslinker. *Cellulose, 21*(3), 1699–1708.

Coseri, S., Biliuta, G., Zemljic, L. F., Srndovic, J. S., Larsson, P. T., Strnad, S., & Lindstrom, T. (2015). One-shot carboxylation of microcrystalline cellulose in the presence of nitroxyl radicals and sodium periodate. *RSC Advances, 5*(104), 85889–85897.

Curvello, R., Mendoza, L., McLiesh, H., Manolios, J., Tabor, R. F., & Garnier, G. (2019). Nanocellulose hydrogel for blood typing tests. *ACS Applied Bio Materials, 2*(6), 2355–2364. https://doi.org/10.1021/acsabm.9b00080.

Curvello, R., Raghuwanshi, V. S., & Garnier, G. (2019). Engineering nanocellulose hydrogels for biomedical applications. *Advances in Colloid and Interface Science, 267*, 47–61.

deNooy, A. E. J., Besemer, A. C., & vanBekkum, H. (1996). On the use of stable organic nitroxyl radicals for the oxidation of primary and secondary alcohols. *Synthesis-Stuttgart,* (10), 1153–1174.

Dufresne, A. (2012). *Nanocellulose: From nature to high performance tailored materials.* De Gruyter.

Dufresne, A. (2013). Nanocellulose: A new ageless bionanomaterial. *Materials Today, 16*(6), 220–227.

Fiorati, A., Contessi Negrini, N., Baschenis, E., Altomare, L., Faré, S., Giacometti Schieroni, A., & Melone, L. (2020). TEMPO-nanocellulose/Ca(2+) hydrogels: Ibuprofen drug diffusion and in vitro cytocompatibility. *Materials (Basel, Switzerland), 13*(1), 183.

Geng, L., Mittal, N., Zhan, C., Ansari, F., Sharma, P. R., Peng, X., & Söderberg, L. D. (2018). Understanding the mechanistic behavior of highly charged cellulose nanofibers in aqueous systems. *Macromolecules, 51*(4), 1498–1506.

Habibi, Y. (2014). Key advances in the chemical modification of nanocelluloses. *Chemical Society Reviews, 43*(5), 1519–1542.

Haun, J. B., Yoon, T.-J., Lee, H., & Weissleder, R. (2010). Magnetic nanoparticle biosensors. *WIREs Nanomedicine and Nanobiotechnology, 2*(3), 291–304.

Hietala, M., Ämmälä, A., Silvennoinen, J., & Liimatainen, H. (2016). Fluting medium strengthened by periodate–chlorite oxidized nanofibrillated celluloses. *Cellulose, 23*(1), 427–437.

Ho, T. T. T., Abe, K., Zimmermann, T., & Yano, H. (2015). Nanofibrillation of pulp fibers by twin-screw extrusion. *Cellulose, 22*(1), 421–433.

Hossain, L., Raghuwanshi, V. S., Tanner, J., Wu, C.-M., Kleinerman, O., Cohen, Y., & Garnier, G. (2020). Structure and swelling of cross-linked nanocellulose foams. *Journal of Colloid and Interface Science, 568*, 234–244.

Hu, J., Tian, D., Renneckar, S., & Saddler, J. N. (2018). Enzyme mediated nanofibrillation of cellulose by the synergistic actions of an endoglucanase, lytic polysaccharide monooxygenase (LPMO) and xylanase. *Scientific Reports, 8*(1), 3195.

Isobe, N., Chen, X. X., Kim, U. J., Kimura, S., Wada, M., Saito, T., ... Isogai, A. (2013). TEMPO-oxidized cellulose hydrogel as a high-capacity and reusable heavy metal ion adsorbent. *Journal of Hazardous Materials, 260*, 195–201.

Isogai, A., Saito, T., & Fukuzumi, H. (2011). TEMPO-oxidized cellulose nanofibers. *Nanoscale, 3*(1), 71–85.

Jiang, J., Ye, W. B., Liu, L., Wang, Z. G., Fan, Y. M., Saito, T., ... Isogai, A. (2017). Cellulose nanofibers prepared using the TEMPO/laccase/O-2 system. *Biomacromolecules, 18*(1), 288–294.

Klemm, D., Schumann, D., Kramer, F., Heßler, N., Koth, D., & Sultanova, B. (2009). Nanocellulose materials - different cellulose, different functionality. *Macromolecular Symposia, 280*(1), 60–71.

Mendoza, L., Batchelor, W., Tabor, R. F., & Garnier, G. (2018). Gelation mechanism of cellulose nanofibre gels: A colloids and interfacial perspective. *Journal of Colloid and Interface Science, 509*, 39–46.

Mendoza, D. J., Browne, C., Raghuwanshi, V. S., Simon, G. P., & Garnier, G. (2019). One-shot TEMPO-periodate oxidation of native cellulose. *Carbohydrate Polymers, 226*, 115292.

Mendoza, L., Gunawardhana, T., Batchelor, W., & Gamier, G. (2018). Effects of fibre dimension and charge density on nanocellulose gels. *Journal of Colloid and Interface Science, 525*, 119–125.

Mendoza, L., Hossain, L., Downey, E., Scales, C., Batchelor, W., & Garnier, G. (2019). Carboxylated nanocellulose foams as superabsorbents. *Journal of Colloid and Interface Science, 538*, 433–439.

Nascimento, D. M., Nunes, Y. L., Figueiredo, M. C. B., de Azeredo, H. M. C., Aouada, F. A., Feitosa, J. P. A., & Dufresne, A. (2018). Nanocellulose nanocomposite hydrogels: technological and environmental issues. *Green Chemistry, 20*(11), 2428–2448.

Okita, Y., Saito, T., & Isogai, A. (2010). Entire surface oxidation of various cellulose microfibrils by TEMPO-mediated oxidation. *Biomacromolecules, 11*(6), 1696–1700.

Perez, D. D., Montanari, S., & Vignon, M. R. (2003). TEMPO-mediated oxidation of cellulose III. *Biomacromolecules, 4*(5), 1417–1425.

Ruizhi, N., Yi, L. L., Yamasaki, S., Lin, J. M., Saito, T., & Isogai, A. (2017). TEMPO-Oxidized Cellulose Nanofiber (TOCN) materials show good biomedical applications. *Abstracts of Papers of the American Chemical Society,* 253.

Saito, T., & Isogai, A. (2004). TEMPO-mediated oxidation of native cellulose. The effect of oxidation conditions on chemical and crystal structures of the water-insoluble fractions. *Biomacromolecules, 5*(5), 1983–1989.

Saito, T., Hirota, M., Tamura, N., Kimura, S., Fukuzumi, H., Heux, L., ... Isogai, A. (2009). Individualization of nano-sized plant cellulose fibrils by direct surface carboxylation using TEMPO catalyst under neutral conditions. *Biomacromolecules, 10*(7), 1992–1996.

Saito, T., Kimura, S., Nishiyama, Y., & Isogai, A. (2007). Cellulose nanofibers prepared by TEMPO-mediated oxidation of native cellulose. *Biomacromolecules, 8*(8), 2485–2491.

Shinoda, R., Saito, T., Okita, Y., & Isogai, A. (2012). Relationship between length and degree of polymerization of TEMPO-oxidized cellulose nanofibrils. *Biomacromolecules, 13*(3), 842–849.

Tarres, Q., Boufi, S., Mutje, P., & Delgado-Aguilar, M. (2017). Enzymatically hydrolyzed and TEMPO-oxidized cellulose nanofibers for the production of nanopapers: Morphological, optical, thermal and mechanical properties. *Cellulose, 24*(9),

3943–3954.
Uetani, K., & Yano, H. (2011). Nanofibrillation of wood pulp using a high-speed blender. *Biomacromolecules, 12*(2), 348–353.
Urena-Benavides, E. E., Ao, G. Y., Davis, V. A., & Kitchens, C. L. (2011). Rheology and phase behavior of lyotropic cellulose nanocrystal suspensions. *Macromolecules, 44*(22), 8990–8998.
Wang, K., & Han, Z. (2017). Injectable hydrogels for ophthalmic applications. *Journal of Controlled Release, 268*, 212–224.
Zander, N. E., Dong, H., Steele, J., & Grant, J. T. (2014). Metal cation cross-linked nanocellulose hydrogels as tissue engineering substrates. *ACS Applied Materials & Interfaces, 6*(21), 18502–18510.
Zhang, K., Feng, W., & Jin, C. (2020). Protocol efficiently measuring the swelling rate of hydrogels. *MethodsX, 7*, 100779.
Zimmermann, T., Pohler, E., & Geiger, T. (2004). Cellulose fibrils for polymer reinforcement. *Advanced Engineering Materials, 6*(9), 754–761.